2021 43rd Annual International Conference of the
IEEE Engineering in Medicine & Biology Society (EMBC)
Oct 31 - Nov 4, 2021. Virtual Conference

A readout circuit realizing electrochemical impedance spectroscopy for FET-based biosensors

Norman Pfeiffer[1], Johannes Rullkötter[1], Christian Hofmann[1], Abdelhamid Errachid[2] and Albert Heuberger[3]

Abstract— **Electrochemical impedance spectroscopy (EIS) is a useful approach for modeling the equivalent circuit of biosensors such as field-effect transistor (FET)-based biosensors. During the process of sensor development, laboratory potentiostats are mainly used to realize the EIS. However, those devices are normally not applicable for real use-cases outside the laboratory, so miniaturized and optimized instrumentations are needed. Various integrated circuits (IC) are available that provide EIS, but these make developed systems highly dependent on semiconductor manufacturers, including component availability. In addition, these generally do not meet the instrumentation requirements for FET-based biosensors, thus external circuitry is necessary as well. In this work, an instrumentation is presented that performs EIS between 10 Hz and 100 kHz for FET-based biosensors. The instrumentation includes the generation of the excitation signal, the configuration of the semiconductor and the readout circuit. The readout circuit consists of a transimpedance amplifier with automatic gain adjustment, filter stages, a magnitude and a phase detection circuit. Since magnitude and phase are converted to a DC signal, digitization of the results is trivial without further signal processing steps, minimizing the computational load on the microcontroller. The transmission behavior of the magnitude and phase measurement circuits shows a high linearity for sinusoidal signals. Furthermore, the overall system was tested with resistors, whereby the magnitude measurement error (1.7%) and the phase shift error (1.6°) were determined within the working range of the instrumentation. The functionality of the instrumentation is demonstrated using pH-sensitive field-effect transistors (ISFET) in various solutions.**

Clinical relevance— **Based on the electrochemical impedance spectroscopy of FET-based biosensors such as ImmunoFETs, new point-of-care testing (POCT) devices can be developed that e.g. quantitatively detect the concentration of biomarkers with very low detection limits in body fluids. The instrumentation presented in this work can be part of new generation of diagnostic tools featuring innovative sensor technologies.**

I. INTRODUCTION

Field-effect transistor (FET) based biosensors were invented 1970 by Bergveld [1] and enjoy increasing popularity since the last 20 years due to the possibility of its fabrication in commercial complementary metal-oxide-semiconductor (CMOS) technologies [2]. Nevertheless, the resulting viable and low-cost mass production of FET-based biosensors and the simple integrability in electronic systems are not the only advantages against other biochemical sensors (e.g. optical sensors) [3]. Furthermore, they enable high sensitivities that even analytes with an amount of substances down to $\mathrm{fmol\,L^{-1}}$ can be detected [4]. Due to the fact that their detection is label-free and provides a fast-response time as well as the possible fabrication on flexible substrates, FET-based biosensors are predestinated as wearable sensors [5].

In the medical field numerous applications of FET-based biosensors are possible, as the evidence of different biomolecular targets are performed. For example, clinical biomarkers for kidney injury, cancers, diabetes, AIDS or cardiovascular diseases can be measured [6], furthermore, the diagnosis of coronavirus disease (COVID-19) using graphene-based FETs has also been demonstrated [7]. Due to its high sensitivity and its low concentration limit, new diagnosis approaches based on unusual body fluids are conceivable like the detection of cardiovascular diseases from saliva samples [8], [9]. Moreover, FET-based gas sensors [10] enable the possibility to use body odours prospectively for diagnosis in addition to liquid substances (e.g. blood, serum, urin, saliva). Because of the shown advantages and its wide range of medical and biochemical applications, FET-based biosensors are a promising technology for future point-of-care testing (POCT).

One way to measure FET-based biosensors is by electrochemical impedance spectroscopy (EIS) [11]. Its advantage is that physical and chemical phenomena on the selective sensor layer of the biosensor can be examined separately from each other. The possible measurement procedures for EIS can be divided into single and multi sine measurements. In the former, excitation signals of different frequencies are sequentially applied to the counter electrode of the sensor and the amplitude and phase of the source current are recorded as the system response. Multi-sine measurements, in contrast, superimpose several sine signals and evaluate the system response in the frequency domain, which can significantly reduce the measurement time. However, the latter suffers from some disadvantages, e.g. the amplitude of the summed excitation signal must not become too high, otherwise nonlinearities may occur when performing an EIS. Low amplitude excitation signals can in turn lead to a low signal-to-noise ratio (SNR) [12].

Expensive and stationary laboratory instrumentation performing EIS is typically used for sensor development, as wide

*This research was funded by EU H2020 research and innovation program entitled KardiaTool with grant Nº 768686.

[1]Norman Pfeiffer, Johannes Rullkötter and Christian Hofmann are with Fraunhofer Institute for Integrated Circuits IIS, 91058 Erlangen, Germany norman.pfeiffer@iis.fraunhofer.de

[2]Abdelhamid Errachid is with Institut des Sciences Analytiques, Université de Lyon, 69100 Villeurbanne, France abdelhamid.errachid-el-salhi@univ-lyon1.fr

[3]Albert Heuberger is with Lehrstuhl für Informationstechnik mit dem Schwerpunkt Kommunikationselektronik (LIKE), Friedrich-Alexander Universität Erlangen-Nürnberg (FAU), 91058 Erlangen, Germany albert.heuberger@fau.de

working ranges and high accuracies are particularly important in enabling comprehensive characterization of biosensors. Not only because of their size, these laboratory devices can no longer be used when biosensors are brought into a concrete application, such as POCT. Therefore, appropriately miniaturized and application-oriented instrumentations are needed.

Several publications have already described electronics for performing EIS that are based on integrated circuits (IC) [13]. Although this has the advantage of miniaturization, it also has the disadvantage of being highly dependent on the manufacturer. Shortages in the supply chains of semiconductor manufacturers have occurred repeatedly in recent years and are expected to continue to occur [14]. This can threaten a planned reproduction project of developed electronics. In contrast, individual components of an analog circuit based on operational amplifiers (OPA) can usually be replaced more easily if they are no longer available or have been discontinued. Additionally, available ICs do not allow complete control of a FET-based biosensor. For example, low frequencies are not supported, the offset voltage of the gate-source voltage cannot be set sufficiently or the drain-source voltage is not provided.

The aim of this work is the design of a readout circuit performing an EIS for FET-based biosensors. This system is designed to both reduce dependence on suppliers of integrated solutions and minimize the computational cost of the embedded system by implementing amplitude and phase detection through analog circuitry rather than digital approaches such as Fast Fourier Transform (FFT). The circuit design is thus chosen in such a way that individual components can be easily replaced by alternatives, depending on requirements or availability, without the need to change the entire architecture or the measurement procedure.

II. METHODS

The readout circuit is controlled and processed by the microcontroller for the realization of the measurement procedure. Individual components and the overall system were evaluated by simulations and measurements with resistors and a pH-sensitive ion-sensitive field-effect transistor (ISFET).

A. Circuit design

To face the disadvantages of using laboratory devices or integrated circuits for impedimetric measurements, a discrete circuit was developed covering a four-channel instrumentation for FET-based biosensors (see Figure 1). The principle block diagram of the circuit is shown in Figure 2 and covers the generation of an excitation signal, a drain voltage supply, a transimpedance amplifier, a precision rectifier, a phase measuring unit and a microcontroller. The instrumentation is supplied by a laboratory power supply with 12 V to ensure large setting ranges for the operating point adjustment of the sensors. However, the implemented measuring principle can also be used with lower supply voltages for battery operation in mobile application scenarios. Since the amplitude and the phase information are converted into a direct current

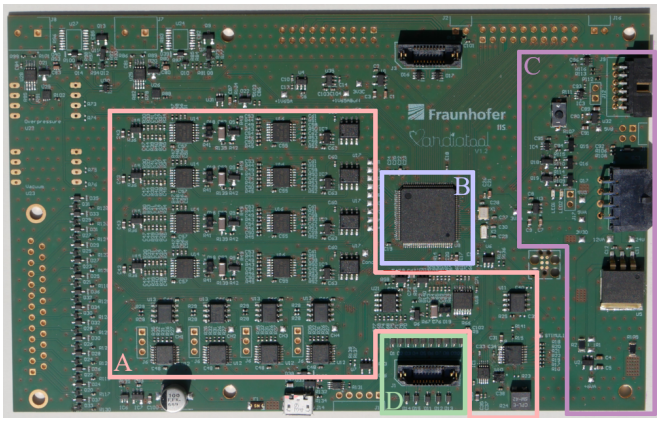

Fig. 1. PCB of the proposed instrumentation: A (red): four-channel analog front end; B (blue): microcontroller STM32F373; C (purple): power management; D (green): terminals for FET-based biosensors; others: various interfaces.

(DC) voltage within the analog domain, no high frequent signals must be digitalized and hence the requirements to the microcontroller can be kept very low. The analog part of one channel is realized with discrete components on an area of about $6\,\mathrm{cm}^2$ on the printed circuit board (PCB).

The presented instrumentation performs an EIS between 10 Hz and 100 kHz. The control of the excitation signal as well as the digitalization of the phase and amplitude information is performed by the microcontroller STM32F373[1].

For setting the operating point of the FET-based biosensor, the excitation signal is not only alternating current (AC) but also superimposed by a DC offset. Therefore, the programmable waveform generator AD9833[2] is used to provide sinusoidal signals up to 100 kHz. The DC component of the excitation signal is generated by the 12-bit digital-to-analog converter (DAC) of the microcontroller and an amplification stage. By using a summation amplifier, both components are superimposed and represent the excitation signal. A potentiostat is used to control the potentials of the reference electrode (RE) and the counter electrode (CE). The drain-source voltage is also controlled via the DAC with amplification stages for each channel.

The readout circuits of the FET-based biosensors are based on a transimpedance amplifier (TIA) converting the drain source-current to a proportional output voltage. In this case, the resistor of the feedback loop determines the factor between input current and output voltage. To ensure a wide working range, not only one but four resistors are switched by an additional multiplexer (MUX) in the feedback loop. Theoretically, currents between a few nanoampere up to 600 µA can be measured with this strategy. Subsequently, active filtering stages realize a bandpass between 1 Hz (first-order high-pass filter) and 300 kHz (second-order low-pass filter). A notch-filter minimizes the coupling of 50 Hz and hence

[1]STM32F373VCT6, STMicroelectronics, Geneva, Switzerland
[2]AD9833BRMZ, Analog Devices, Massachusetts, USA

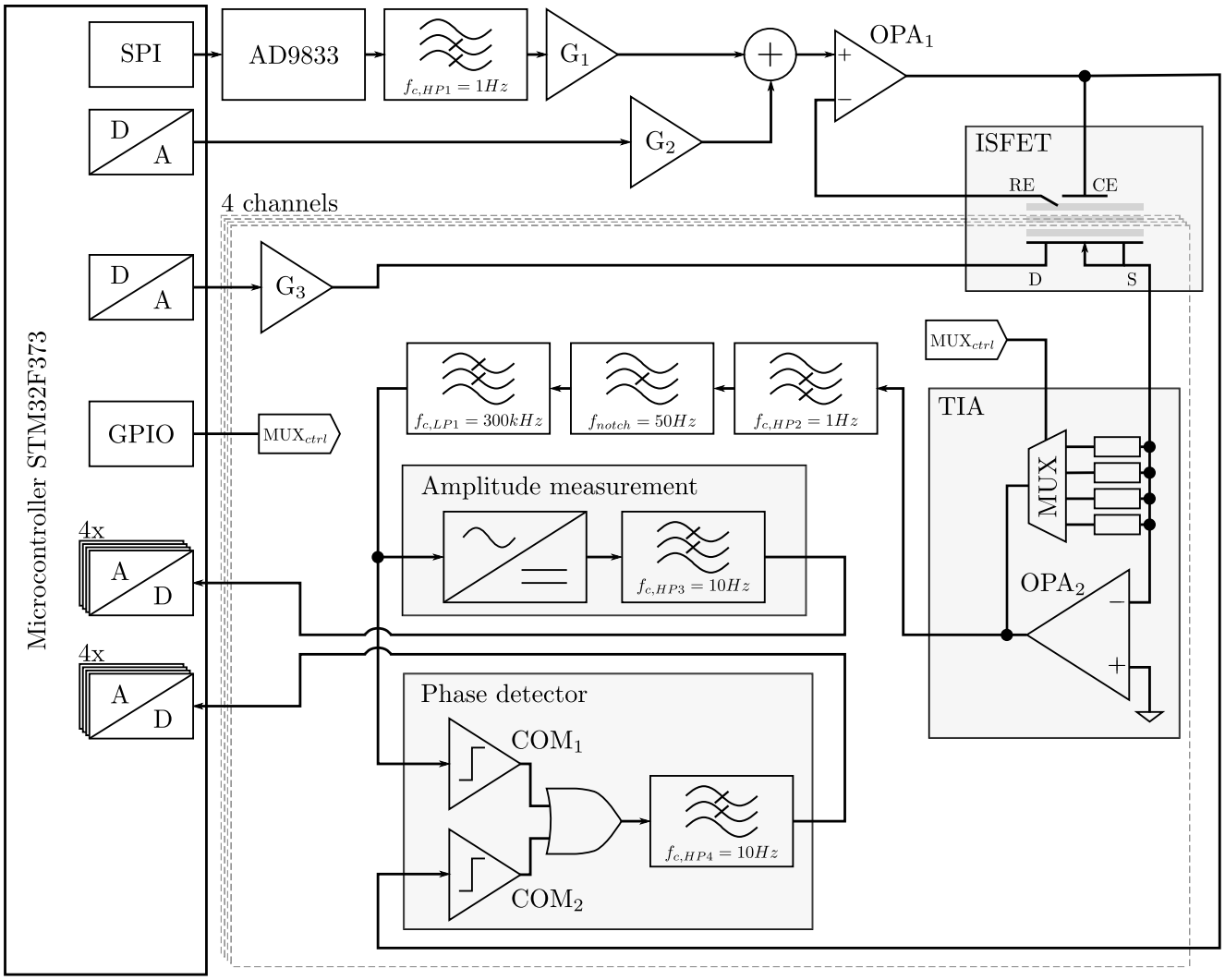

Fig. 2. Block diagram of the discrete circuit realizing a four-channel impedance spectroscopy. The generation of the excitation signal (sine wave) is performed by the AD9833. After amplification and superimposing with a DC voltage, this signal is applied to the counter (CE) and reference electrode (RE) by means of a potentiostat. For each of the four FET-based biosensors, the drain-source voltage U_{ds} is generated and applied to the drain (D). The drain current I_d is acquired from the sources S and amplified by individual transimpedance amplifiers (TIA). Subsequently, the amplitudes and phase information are transformed into DC voltages, which can be easily digitized by the microcontroller's ADCs.

prevents a modulation of the useful signal enabling the usage of this instrumentation for small currents without additional Faraday cage. The latter is often used to minimize electrical interference (e.g. 50 or 60 Hz hum) on the electrochemical cell and its leads. However, the disadvantage of the notch filter is that the detection of the affected part of the spectrum is impeded.

In order to implement the magnitude measurement of the sinusoidal signal a peak rectifier is used (see Figure 3). The diodes D_1 and D_2 and the operational amplifier $\mathrm{OPA_{A1}}$ rectify the input signal. This signal charges capacitor C_1 to the maximum voltage. As it is only discharged very slowly via the resistor R_3, the voltage is stored in C_1. The transistor Q_1 blocks during the measurement process, which means that no discharge current can flow. $\mathrm{OPA_{A2}}$ is used as an impedance converter. If C_1 is incorrectly charged to a high voltage due to interference coupling, it can be discharged via Q_1 by the microcontroller. The resistor R_1 prevents the operational amplifier $\mathrm{OPA_{A1}}$ from being driven into saturation. As a result, the output voltage of the peak rectifier is a DC voltage, which is digitized by the analog-to-digital converter (ADC) of the microcontroller. As a reference, the magnitude of the excitation signal itself is also measured by a fifth channel.

For phase detection, the measurement and the reference signal are transformed into square-wave signals by means of analog comparators with virtual ground at the positive inputs and the sine waves at the negative inputs. These square-wave signals represent a high level for the positive half-wave of a sinusoidal signal. Both square-wave signals are then processed by an XOR gate whose output signal has high-periods proportional to the phase shift between $0°$ and $180°$. A low-pass filter is used to obtain a DC output voltage.

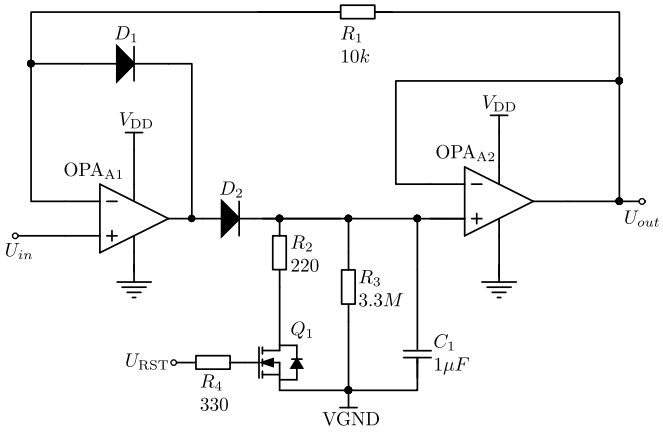

Fig. 3. Amplitude measurement circuit based on a peak rectifier.

B. Measuring procedure

The measuring procedure is shown as a flow chart in Figure 4. A measurement can be initialized via an universal serial bus (USB) 2.0 full speed connection. Thus, commands can be sent to the microcontroller to configure various measurement parameters or to perform a measurement with specified parameters. Adjustable parameters include frequency (10 Hz - 100 kHz), gate-source offset voltage (± 2.5 V), drain-source voltage (<6 V) and settling time (<5 s). Due to the adjustability of the different parameters, the control of different sensor front ends is possible, so that the device can be used for a wide range of applications. At the beginning of a measurement the microcontroller transmits the next excitation frequency via serial peripheral interface (SPI) to the frequency generator AD9833 and activates its output. Afterwards, the five magnitude measurement circuits are reset by activating the transistor Q_1 and the MUX in the feedback loop of the TIA switches to the resistor with the lowest amplification. For digitalization of the DC outputs generated by the amplitude and phase measurements, one ADC of the microcontroller is used for each. The signals are recorded with a sampling frequency of 100 Hz and written to the memory via Direct Memory Access (DMA). This relieves the main processor of the microcontroller so that the computing power is available for other purposes or the microcontroller is able to enter a sleep mode. Since the measurement can be affected by a transient response, a settling time is considered prior to each measurement.

Before starting the actual measurement for a specific frequency, the system performs a gain adjustment. At the starting point, all measuring resistors are set to the smallest value. With these resistors a defined number of amplitude samples are measured and then averaged for each channel. These values are then used to check whether the channels are in saturation or whether the amplitude of the measurement signal is very low. The next resistor is set depending on the mean value being larger or smaller than the defined limits. The resistor is kept if the mean value is within the limits. This process is performed before each frequency measuerment, which increases the measurement time, but ensures that the measurement can be performed over large impedance ranges. Finally, the magnitude and phase measurement is performed again with the appropriate gain. The obtained measured values are sent to a PC via USB.

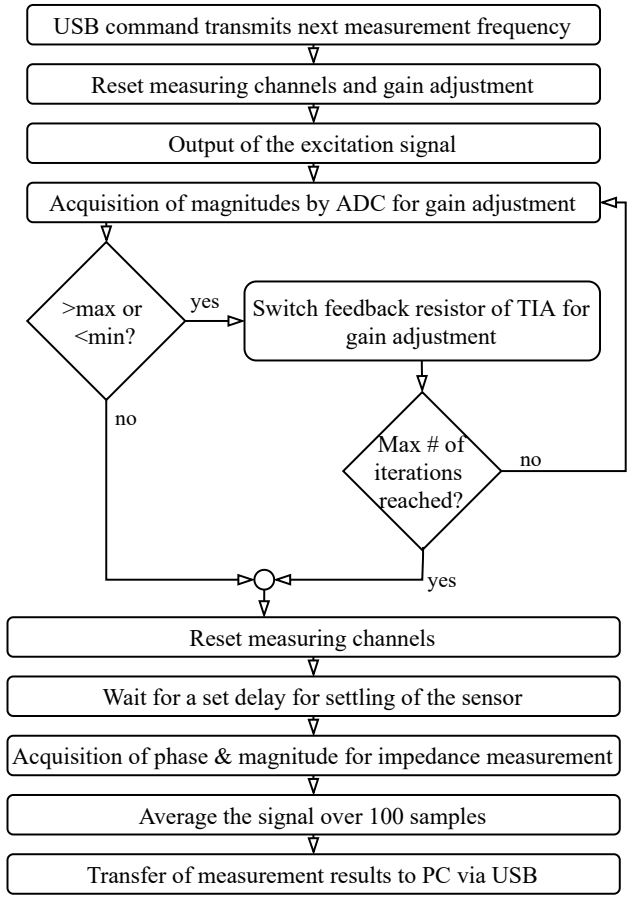

Fig. 4. Flowchart of impedance acquisition for one frequency. During gain adjustment, the measurement signal is compared with a minimum and maximum threshold and adjusted accordingly. After a maximum of 3 iterations, the gain adjustment is terminated.

C. Evaluation

To verify the principal functionality and to evaluate frequency dependencies, the phase and magnitude measurements were simulated through transient analysis by the software LTSpice. Both input sinusoidal signals were set to a magnitude of 1 V for the phase detector. Additionally, in order to investigate how the circuits react to distortions of the sinusoidal signal, which may possibly occur due to the non-linear behavior of the FET-based biosensor, a 100 Hz sinusoidal signal was exemplarily superimposed with its second harmonic. The amplitudes of these two frequency components were equal and were chosen so that the resulting amplitude was equal to that of the non-superimposed sinusoidal signal.

In order to analyze the transfer behavior of the overall system, real measurements were made using 10 kΩ, 100 kΩ and 1 MΩ resistors. For this purpose, the terminals of RE and CE were short-circuited and the resistors were connected between CE

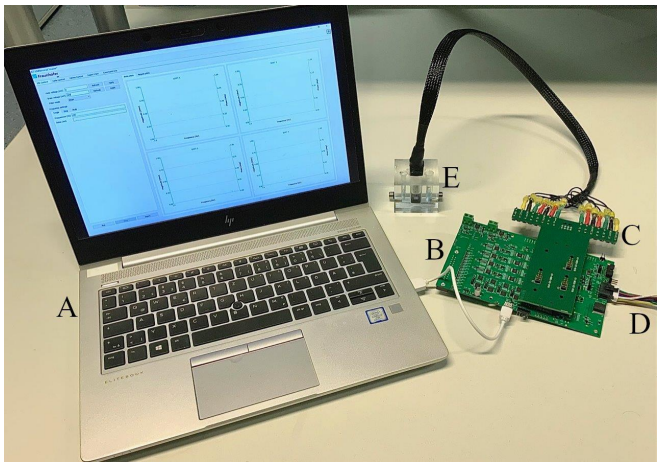

Fig. 5. Measurement setup for the usage of a 4-channel ISFET in pH solutions. A: PC with software for configuration of the instrumentation and recording of the spectra; B: Presented instrumentation; C: Adapter board for cable connection; D: Voltage supply leads; E: Electrochemical cell with ISFETs.

and source terminal. In this test scenario, no offset voltage was superimposed on the excitation signal and the drain voltage was not applicable.

As shown in Figure 5, the overall system was finally tested on a pH-sensitive 4-channel ISFET produced at the Institute of Miroelectronics of Barcelona (IMB-CNM) of the Spanish National Research Council (CSIC). Detailed descriptions of the sensor have already been published and can be obtained from [15]. The application of a similar sensor has already been demonstrated with EIS and the concentration-dependent shift of the threshold voltage [8], [9]. Exemplary measurements were performed with the integrated platinum counter electrode of the sensing chip and solutions of pH 4, pH 7 and pH 9.

III. RESULTS

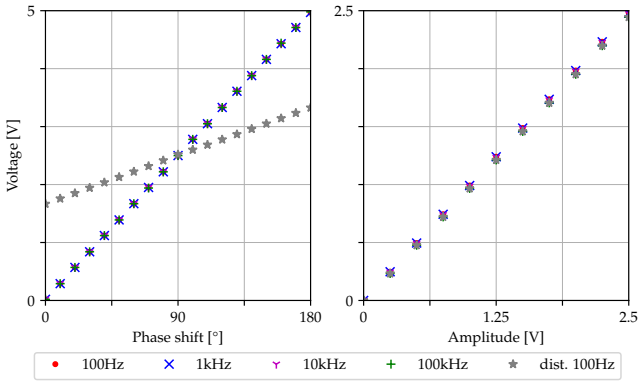

Fig. 6. Simulation results generated with LTSpice; Left: Response of the phase detector circuit; Right: Response of the amplitude measurement circuit; Both circuits show a linear behaviour with sinusoidal input signals. Distorted sinusoidal signals (here: 100 Hz with its second harmonic) interferes with the phase measurement.

Figure 6 shows the linear relationship between phase shift and output voltage of the phase detector circuit for frequencies between 10 Hz and 100 kHz. The maximum output voltage at 180° is equal to the supply voltage of the comparators. The response of the magnitude measurements also shows a linear behaviour for the same frequency range. When using a distorted sinusoidal signal, the influence on the magnitude measurement is marginal, but it has a considerable impact on the phase measurement. In the examined case, the behavior is still linear, but with a different slope, which hinders the detection of the correct phase shift.

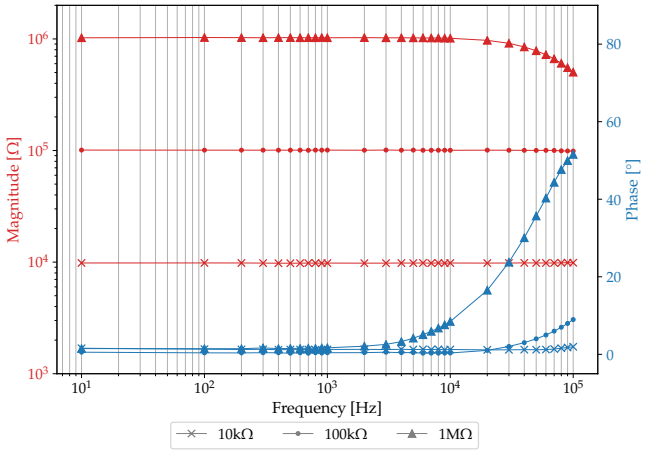

Fig. 7. Frequency response (red: magnitude, blue: phase) of the overall circuit considering various resistances between 10 kΩ and 1 MΩ. At high resistances, low-pass behavior occurs due to parasitic capacitance of the TIA.

The frequency response of the overall circuit is shown by means of the measurement of various resistances in Figure 7. It can be shown that at low frequencies the impedance measurement can be carried out accurately (error of magnitude measurement $< 1.7\%$ and error of phase shift $< 1.6°$). In this measurement range, the achieved accuracies are comparable to other portable systems [16]. However, it turns out clearly that the circuit exhibits attenuation for high amplitudes and high frequencies due to parasitic capacitances at the first amplifier stage and is therefore not suitable for impedance measurements in this range. Frequencies around 50 Hz were omitted for the measurements shown, as these would be influenced by the notch filter used.

Examples of the response while measuring pH with ISFETs is shown in Figure 8. The following parametrization is used: drain-source voltage $U_{ds} = 500\,\mathrm{mV}$, DC of the gate-source voltage $U_{gs,dc} = -200\,\mathrm{mV}$, amplitude of the alternating part of the gate-source voltage $U_{gs,ac} = 42\,\mathrm{mV}$. For both solutions the sensor follows the electrical equivalent circuit of a Randles circuit. The relationship between the charge transfer resistance R_{ct} and the pH value appears through the enlargement of the diameter of the semicircle. The fitting of the Randles Circuit's semicircle in Figure 8 was performed as presented in [17].

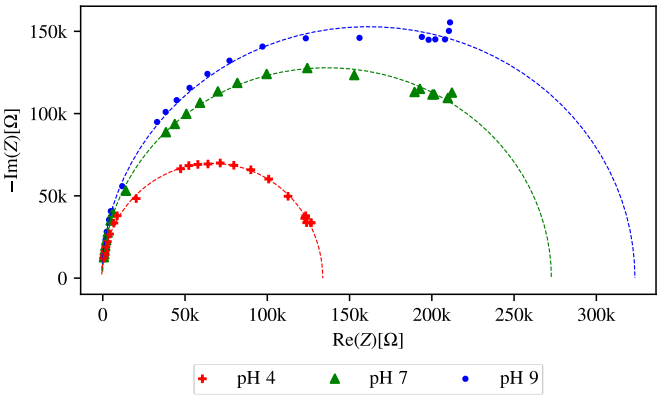

Fig. 8. Example of Nyquist plots showing the electrical behaviour of a Randles Circuit for pH sensitive ISFET for pH4 (red), pH 7 (green) and 9 (blue).

IV. DISCUSSION

The presented measurement system provides an alternative approach to the available integrated solutions and can be replicated and adopted to other applications with low development effort compared to a semiconductor development. Signal evaluation is performed in the analog domain, which minimizes the computing effort of the microcontroller. Only the signal generation is done by the IC AD9833, but in next versions it can alternatively be realized directly by the DAC of the microcontroller to minimize the number of components. The simulations demonstrate that the presented measurement system can be used by ensuring that the sensor under investigation has a linear response. This is for example achieved by keeping the amplitude of the excitation signal for EIS as low as possible. However, as soon as a distorted sine wave is to be detected, the phase detection circuit in particular can lead to errors.

As generally known with impedance measurement systems, high impedances cannot be measured reliably at high frequencies. This behavior is mainly caused by the TIA, since parasitic capacitances can lead to low-pass characteristics. To counteract this behaviour, various parasitic capacitances should be reduced in further designs, such as the input capacitance of the OPA, parasitic capacitances due to leads or input / output capacitances of the MUX in the feedback. Alternatively, calibrations can be used to correct the response for high frequencies and large impedances. However, since the presented system is primarily intended to measure FET-based biosensors whose equivalent circuit is described by the Randles Circuit, high impedances at high frequencies are not expected. In future research, this should be evaluated on specific applications with biofunctionalized sensors and corresponding samples.

To minimize the number of components, future work has to consider the use of MUXs at the sensor terminals to acquire multi-channel measurements sequentially through a single-channel circuit. Limiting influences in this context may be parasitic capacitances or leakage currents.

REFERENCES

[1] P. Bergveld, Short Communications: Development of an Ion-Sensitive Solid-State Device for Neurophysiological Measurements, IEEE Transactions on Biomedical Engineering, vol. BME-17, no. 1, pp. 70-71, 1970

[2] J. Bausells, J. Carrabina, A. Errachid and A. Merlos, on-sensitive field-effect transistors fabricated in a commercial CMOS technology, Sensors and Actuators, B: Chemical, vol. 57, no. 1-3, pp. 56-62, 1999

[3] M. Dei, J. Aymerich, M. Piotto, P. Bruschi, F. J. del Campo, F. Serra-Graells, CMOS interfaces for internet-of-wearables electrochemical sensors: trends and challenges, Electronics (Switzerland), vol. 8, no. 2, pp. 1-42, 2019

[4] A. Nehra and K. Pal Singh, Current trends in nanomaterial embedded field effect transistor-based biosensor, Biosensors and Bioelectronics, vol. 74, pp. 731-743, 2015

[5] A. Yasuda and W. Knoll, Organic Bioelectronics for Life Science and Healthcare, Materials Research Forum LLC, 2019

[6] Y. C. Syu, W. E. Hsu and C. T. Lin, Review-field-effect transistor biosensing: Devices and clinical applications, ECS Journal of Solid State Science and Technology, vol. 7, no. 7, pp. Q3196-Q3207, 2018

[7] J. Sengupta and M. Hussain, Graphene-based field-effect transistor biosensors for the rapid detection and analysis of viruses: A perspective in view of COVID-19, Carbon Trends, vol. 2, 100011, 2021

[8] D. Vozgirdaite, H.B. Halima F.G. Bellagambi, A. Alcacer, F. Palacio, N. Jaffrezic-Renault, N. Zine, J. Baussels, A. Elaissari and A. Errachid, Development of an ImmunoFET for Analysis of Tumour Necrosis Factor-α in Artificial Saliva: Application for Heart Failure Monitoring, J Chemosensors, vol. 9, no. 2, pp. 26, 2021

[9] B. H. Hamdi, G. B. Francesca, A. Alcacer, N. Pfeiffer, A. Heuberger, M. Hangouët, N. Zine, J. Bausells, A. Elaissari and A. Errachid, A silicon nitride ISFET based immunosensor for Tumor Necrosis Factor-alpha detection in saliva. A promising tool for heart failure monitoring, Analytica Chimica Acta, p. 338468, 2021

[10] S. Hong, M. Wu, Y. Hong, Y. Jeong, G. Jung, W. Shin, J. Park, D. Kim, D. Jang and J.-H. Lee, FET-type gas sensors: A review, Sensors and Actuators B: Chemical, vol. 330, 129240, 2021

[11] A. B. Kharitonov, The Use of Impedance Spectroscopy for the Characterization of Protein-Modified ISFET Devices: Application of the Method for the Analysis of Biorecognition Processes, The Journal of Physical Chemistry B 105, no. 19, pp. 4205-4213, 2001

[12] J. Ojarand, P. Annus, M. Min, M. Gorev and P. Ellervee, Optimization of multisine excitation for a bioimpedance measurement device, 2014 IEEE International Instrumentation and Measurement Technology Conference (I2MTC) Proceedings, pp. 829-832, 2014

[13] K. Charbowski, T. Piasecki, A. Dzierka and K. Nitsch, Simple Wide Frequency Range Impedance Meter Based on AD5933 Integrated Circuit, Metrology and Measurement Systems, vol. 22, no. 1, pp. 13-24, 2015

[14] Oxford Analytica, The semiconductor demand/supply imbalance will persist, Expert Briefings, 2021

[15] A. Alcacer, B. H. Hamdi, M. Hangouët, H. ElAissari, A. Errachid and J. Bausells, eHealth system with ISFEET-based immunosensor for heart failure biomarker detection in saliva, 13th Spanish Conference on Electron Devices (CDE). IEEE, pp 114-116, 2021

[16] A. A. Al-Ali, B. J Maundy and A. S. Elwakil, Design and implementation of portable impedance analyzers, Springer International Publishing, 2019

[17] N. Pfeiffer, T. Wachter, J. Frickel, C. Hofmann, A. Errachid and A. Heuberger, Elliptical Fitting as an Alternative Approach to Complex Nonlinear Least Squares Regression for Modeling Electrochemical Impedance Spectroscopy, Proceedings of the 14th International Joint Conference on Biomedical Engineering Systems and Technologies - Volume 2: BIOSIGNALS, pp 42-49, 2021